Fish and Shellfish Immunology 94 (2019) 661–674

Contents lists available at ScienceDirect

Fish and Shellfish Immunology

journal homepage: www.elsevier.com/locate/fsi

Full length article

Skin metabolome reveals immune responses in yellow drum *Nibea albiflora* to *Cryptocaryon irritans* infection

Ivon F. Maha[a,b,1], Xiao Xie[a,b,1], Suming Zhou[a,b], Youbin Yu[a,b], Xiao Liu[a,b], Aysha Zahid[a,b], Yuhua Lei[a,b], Rongrong Ma[a,b], Fei Yin[a,b,*], Dong Qian[a,b,**]

[a] Key Laboratory of Applied Marine Biotechnology, Ministry of Education, Collaborative Innovation Centre for Zhejiang Marine High-efficiency and Healthy Aquaculture, Ningbo University, 818 Fenghua Road, Ningbo, 315211, PR China
[b] School of Marine Sciences, Ningbo University, 169 South Qixing Road, Ningbo, 315832, PR China

ARTICLE INFO

Keywords:
Metabolomics
Cryptocaryon irritans
Nibea albiflora
Skin

ABSTRACT

The yellow drum *Nibea albiflora* is less susceptible to *Cryptocaryon irritans* infection than is the case with other marine fishes such as *Larimichthys crocea*, *Lateolabrax japonicus,* and *Pagrus major*. To investigate further their resistance mechanism, we infected the *N. albiflora* with the *C. irritans* at a median lethal concentration of 2050 theronts/g fish. The skins of the infected and the uninfected fishes were sampled at 24 h and 72 h followed by an extensive analysis of metabolism. The study results revealed that there were 2694 potential metabolites. At 24 h post-infection, 12 metabolites were up-regulated and 17 were down-regulated whereas at 72 h post-infection, 22 metabolites were up-regulated and 26 were down-regulated. Pathway enrichment analysis shows that the differential enriched pathways were higher at 24 h with 22 categories and 58 subcategories (49 up, 9 down) than at 72 h whereby the differential enriched pathways were 6 categories and 8 subcategories (4 up, 4 down). In addition, the principal component analysis (PCA) plot shows that at 24 h the metabolites composition of infected group were separately clustered to uninfected group while at 72 h the metabolites composition in infected group were much closer to uninfected group. This indicated that *C. irritans* caused strong metabolic stress on the *N. albiflora* at 24 h and restoration of the dysregulated metabolic state took place at 72 h of infection. Also, at 72 h post infection a total of 17 compounds were identified as potential biomarkers.

Furthermore, out of 2694 primary metabolites detected, 23 metabolites could be clearly identified and semi quantified with a known identification number and assigned into 66 Kyoto Encyclopedia of Genes and Genomes (KEGG) pathways. Most of the enriched KEGG pathways were mainly from metabolic pathway classes, including the metabolic pathway, biosynthesis of secondary metabolites, taurine and hypotaurine metabolism, purine metabolism, linoleic acid metabolism, phenylalanine, tyrosine and tryptophan biosynthesis. Others were glyoxylate and dicarboxylate metabolism, glutathione metabolism, and alanine, aspartate, and glutamate metabolism. Moreover, out of the identified metabolites, only 6 metabolites were statistically differentially expressed, namely, L -glutamate (up-regulated) at 24 h was important for energy and precursor for other glutathiones and instruments of preventing oxidative injury; 15-hydroxy- eicosatetraenoic acid (15-HETE), (S)-(−)-2-Hydroxyisocaproic acid, and adenine (up-regulated) at 72 h were important for anti-inflammatory and immune responses during infection; others were delta-valerolactam and betaine which were down-regulated compared to uninfected group at 72 h, might be related to immure responses including stimulation of immune system such as production of antibodies.

Our results therefore further advance our understanding on the immunological regulation of *N. albiflora* during immune response against infections as they indicated a strong relationship between skin metabolome and *C. irritans* infection.

* Corresponding author. Key Laboratory of Applied Marine Biotechnology, Ministry of Education; Collaborative Innovation Centre for Zhejiang Marine High-efficiency and Healthy Aquaculture, Ningbo University, 818 Fenghua Road, Ningbo 315211, PR China.
** Corresponding author. School of Marine Sciences, Ningbo University, 169 South Qixing Road, Ningbo 315832, PR China.
E-mail addresses: yinfei@nbu.edu.cn (F. Yin), qiandong@nbu.edu.cn (D. Qian).
[1] The authors contributed equally to this work.

https://doi.org/10.1016/j.fsi.2019.09.027
Received 3 June 2019; Received in revised form 28 August 2019; Accepted 12 September 2019
Available online 12 September 2019

1. Introduction

Cyptocaryoniasis in marine fish is a major cause of massive deaths in aquaculture and it can therefore cause a high loss of output and economic values [1,2]. Cyptocaryoniasis is caused by *Cryptocaryon irritans,* a ciliated protozoan parasite which parasitizes in the epithelial tissue of skin, gill, and fins causing small white spots and nodules on the locally infected parts [3]. The *C. irritans* is known to cause diseases in many fish species, although at a different range of harm effect [3]. Several studies [4–8] revealed that *Nibea albiflora* is less susceptible to *C. irritans* than is the case with other marine fishes such as *Larimichthys crocea*, *Lateolabrax japonicus,* and *Pagrus major*. In addition, challenged *N. albiflora* with *C. irritans* showed immunological resistant against cyptocaryoniasis [6].

In order to find out the mechanism of immune tolerance of fish against pathogens, the researchers carried out studies at physiology, biochemistry, and molecular biology levels [9–11]. In recent years, genomic, transcriptomic, and proteomic technologies are extensively used because of the advancement of high-throughput sequencing technology [12–15]. In addition, low molecular weight metabolites are the final product of gene expression, therefore their levels can be considered as a powerful approach in evaluating the responses of a living system to pathophysiological stimuli in detecting the changes of metabolites in biological samples such as somatic cells, tissues, or fluids [16,17]. For that reason, metabolomics is an important tool of identifying vital biomarkers which are responsible for metabolic attributes, and of disclosing metabolic mechanisms during infections [18]. These biomarkers are able to redirect a metabolome and thereby enabling them to fight against the host environmental changes and pathogen attack [19,20]. Furthermore, fish can produce mediators that comprise metabolites to instigate inflammatory process as an integral part of the innate immune system that aims at restricting, reducing, and ending the infection [21]. For example, metabolites such as L-valine can be immunoregulators that alter the function of immune cells [22]. Therefore, metabolomics is potentially useful in the monitoring of disease-causing agents, using the corresponding metabolite biomarkers, as it illustrates the alteration in metabolites that participated in the same metabolic pathway [23,24]. Furthermore, we can use these metabolic biomarkers in the explorationof the ways of enhancing innate immune responses because using metabolites from organisms themselves, has low antigenicity and little or even no toxicity to the organism [25].

Metabolomics studies on essential biomarkers in their immune responses in different aquatic organisms have been done. These studies have shown that Pacific white shrimp *Litopenaeus vannamei* whereby the White spot syndrome virus (WSSV) disease caused the absorption inhibition of amino acids, disturbance in protein metabolism, and cell metabolism in favour of its replication [26]. In addition, *Vibrio anguillarum* and *V. splendidus* infection were reported to stimulate disturbances in energy metabolism and osmotic regulation, and oxidative and immune stresses in Clam *Ruditapes philippinarum* [27]. Moreover, the *V. harveyi* infection in Manila clam *R. philippinarum* was reported to induce a disturbance in energy metabolism and immune stresses in both White and Zebra clam hepatopancreas [28]. In addition, the study on metabolic responses of abalones *Haliotis diversicolor,* which was infected by *V. parahemolyticus* caused an interruption in energy metabolism, nucleotide metabolism, osmotic balance, induce oxidative stress, immune stress, and neurotoxic effect in different tissues [29]. Furthermore, a metabolomic study in tilapia *Oreochromis niloticus* which was infected by *Streptococcus iniae* showed that N-acetylglucosamine could significantly elevate the survival of tilapia against *S. iniae* infection [30].

Apart from these efforts, to the best of our knowledge, no surveys have been undertaken to examine the reactions induced by *C. irritans* in the skin of marine fish using a metabolomic approach. The skin is the largest organ, and functionally it is in direct contact with the environment and provides the first defence barrier against stressors including parasites [11]. Therefore, we employed non-targeted liquid chromatography-mass spectrometry (LC-MS) metabolomic approach to study the responsive profiles in the skin of *N. albiflora* which was infected with *C.irritans.* Since the disease symptom starts at 24 h post-infection and the trophonts start shedding from the infected fish after 72 h post-infection [4,5,7], therefore, to avoid reinfection we selected two-time points, which are 24 h and 72 h for our study. Our hypothesis was that the skin metabolome reflects a metabolic strategy against *C. irritans* infection, which is responsible for the body immunity.

2. Materials and methods

2.1. Cryptocaryon irritans

C. irritans were obtained from the naturally diseased *L. crocea* (100 ± 10 g) and transferred into the container for the *C. irritans* propagation with the same fish species according to Yin *et al.* procedure [7]. Briefly, twenty healthy *L. crocea* were selected and maintained in a 1000-L aquarium. The experimental animals *L. crocea* were infected with a non-lethal concentration of theronts (10,000 theronts/fish), in 5 L of seawater per fish. After 2 h post-infection in the dark, fresh seawater was added for maintaining standard culture condition. After three to four days, tomonts were found at the bottom of the *L. crocea* culture aquarium. The infected fishes were transferred to another clean aquarium without tomonts. Using a banister brush, the tomonts were carefully collected from the bottom of the aquarium and placed into a 1L beaker for incubation. After two to three days of incubation, active *C. irritans* theronts that had hatched for no more than 2 h were collected and their concentration was calculated according to Dan *et al.* procedure before the infection examination [31].

2.2. Experimental fish

Healthy *N. albiflora* with an average body weight of 40 ± 3g and body length of 13.3 ± 0.3 cm were obtained from fish farms in Fuding City, Fujian Province, in China. Samples of 10 fishes were randomly selected and examined; no parasites were identified on their gills, fins, or skin. The selected fishes were acclimatized for one week prior to infection. Artificial breeding was performed in a 1062 L (ϕbottom = 130 cm × H = 80 cm) fiberglass aquarium. The fishes were fed twice a day (8:00 and 15:00) with commercially produced feed. Water quality and other environmental conditions such as water salinity, temperature, light intensity, and photoperiod for both the propagation and the experiment were 29–32‰, 27 ± 1 °C, 1000 lx, and 12 L: 12 D, respectively.

2.3. Experimental methods

Ninety *N. albiflora* were challenged with *C. irritans* theronts which were hatched for no more than 2 h at a dose of 2050 theronts per gram of fish as per Yin et al. procedure [5]. The infection took place in a 1062 L fiberglass aquarium with 2 L of water for each fish. The infection lasted for 2 h in the dark, and then clean seawater was added. Another 90 healthy fish were treated in the same manner but they were not treated with the parasite as the control group. After 24 h post-infection, the group of infected and the uninfected fish were then changed to other clean 344 (ϕbottom = 74 cm × H = 80 cm) fiberglass aquariums without parasites as followed by Yin *et al.* [5]. Each group contained 6 parallel subgroups (15fish/aquarium). The experiment lasted for 72 h.

2.4. Skin samples collection

After 24 h and 72 h post-infection, 9 fish from each group were sampled and anesthetized with buffered tricaine methanesulfonate (MS-222; 100 mg/L buffered with 200 mg NaHCO3/L; Finquel, Argent, Redmond, WA). They were sacrificed and skinned by using a sterilized

knife. The skin samples were immediately flash-frozen in liquid nitrogen and stored at −80 °C in the laboratory until further processing.

2.5. LC–MS-based metabolome analysis

Polar metabolites were extracted from the skin sample using a two-step biphasic extraction, methanol/chloroform/water as per Wu et al. procedure [32]. Briefly, the skin sample of about 50 mg was homogenized in 4 mL/g of cold methanol and 0.85 mL/g of cold water by a TissueLyser LT bead mill (Qiagen) with 3.2 mm stainless steel beads, for 10 min at 50vibrations/s. The homogenates were moved into glass vials; 4 mL/g chloroform and 2 mL/g water were added. The samples were vortexed, left on ice for 10 min for phase separation, and centrifuged for 5 min at 2000 g at 4 °C. A 600 μL volume of the upper methanol layer containing the polar metabolites was transferred into glass vials, dried in a centrifugal vacuum concentrator (Eppendorf 5301), and stored at −80 °C prior to liquid chromatography-mass spectrometry (LC-MS) analysis. The LC-MS analysis of the metabolomics sequence was performed as followed by Ekman *et al.* [33].

2.6. Differential metabolite pathways

The pathway activity profiling (PAPi) algorithm was used to calculate the activity score (AS) for each metabolic pathway based on the number and relative abundance of each metabolic pathway in the Kyoto Encyclopedia of Genes and Genome (KEGG) database degree. Important features were recognized using Bio Deep analysis software, an online database for annotation of metabolites developed by IntelliCAM. The database was set to filter out metabolites which do not fall under the specified ± 0.001% difference in the *m/z* values were used as followed by Sotto et al. [34]. The identification of parent ions was performed in the full scan mode by recording from 50 to 800 (*m/z*) in both positive and negative ionization modes.

2.7. Multivariate statistical analysis

Data were analysed using the Soft Independent Modelling by Class Analogy (SIMCA) software SIMCA-P (V13. 0) as previously performed by Liu *et al.* and Lu et al. [26,29]. The supervised multivariate data analysis methods, the principal component analysis (PCA), the partial least squares discriminant analysis (PLS-DA), and (OPLS-DA) were sequentially used to uncover and extract the statistically significant metabolite.

The two-way analysis of variance (ANOVA) using SPSS (V22.0) with Tukey's test was conducted on the metabolite concentrations from both infected anduninfected groups to test the possible metabolic differences induced by the *C. irritans* in the skin of *N. albiflora*. All the metabolite concentrations were shown as means ± standard deviation (mean ± S.D.) A p value of less than 0.05 was considered significant.

3. Results

In order to evaluate metabolic responses between the groups, we investigated metabolite changes in the skin following the *C. irritans* infection. A total of 2694 potential metabolites, 980 from positive ionization mode, and 1714 from negative ionization mode were identified. Then, the plot was drawn total ion chromatogram (TIC), A for positive ionization mode and B for negative ionization mode). The ionic strength for the vertical axis and time for the abscissa, which could directly show the differences in the metabolite profiles among the groups, were recorded (Fig. 1 A and B).

The PCA were clustered into two groups (Fig. 2A and B), followed by supervised analysis techniques the OPLS-DA so as to maximize the difference between the two groups and assist in the viewing of the marker metabolites, which are liable for class separation by removing systematic variations [35]. In order to distinguish further the *C. irritans* infected groups and the uninfected groups, the OPLS-DA models were analysed (Fig. 2C and D). For positive (A) ion, at 24 h post-infection, we discriminated the 24 h-infected and the 24 h-uninfected group subjects with R2X of 25.7%, an R2Y of 96.3%, and Q2 of 63.7%. At 72 h, we discriminated the 72 h-infected and the 72 h-uninfected group subjects with an R2X of 38.8%, an R2Y of 1% and a Q2 of 70.9%. On the other hand, when the 72 h-infected and 24 h-infected groups were compared, we discriminated the group subjects with an R2X of 35.5%, an R2Y of 99.9%, and a Q2 of 72.1%, whereby, R2 and Q2 indicate high goodness of fit and a high percentage of prediction, respectively.

For negative ion (B) at 24 h postinfection, we discriminated the 24 h-infected and 24 h-uninfected groups subject with R2X of 37.7%, an R2Y of 1% and a Q2 of 50.1%. At 72 h, we discriminated the 72 h-infected and the 72 h-uninfected groups subject with an R2X of 36.7%, an R2Y of 1% and a Q2 of 38.3%. On the other hand, when the 72 h-infected and 24 h-infected groups were compared, we discriminated the group subjects with an R2X of 35.2%, an R2Y of 1% and a Q2 of 26.6%, whereby, R2 and Q2 indicate high goodness of fit and a high percentage of prediction, respectively. The OPLS-DA of 100 Y-permutated models were visualized in validation plots as tabulated in (Table 1). Finally, we screened out the differential metabolites (biomarkers) by selecting metabolites with high s-plot, P-value and P corr at P-value ≤ 0.05 + VIP > = 1 + s-plot. P corr ≥0.8 and finally, the S-plot were plotted (Fig. 3 A and B). The closer the metabolites to the lower left (left bottom) and upper right (top right) the greater they contribute to the difference between treatments. At the positive ionization mode, 8 compounds were idetified as biomarkers at 72 h. These include the compounds with number 818, 835, 868, 859, 831,834,951,and 864 (Table S2). While at the negative ionization mode 9 compounds were identified as biomarkers at 72 h. These include the compounds with number 284, 294, 907,984, 985, 1017, 1025, 1686, and 9842(Table S3).

3.1. Metabolic changes in the skin after C. irritans treatments

After infection, the fish skin metabolites showed significant up and down-regulation. A pairwise group comparison between the infected and the uninfected groups at 24 h and 72 h post-infection was carried out to assess the difference in metabolites. Out of 2694 primary metabolites detected, only 135 metabolites were differentially expressed. At positive (A) ionization mode during 24 h post-infection, 5 metabolites were up-regulated and 15 were down-regulated in the infected groups (Fig. 4A). At negative ionization mode (B) ion, 7 metabolites were up-regulated and 2 were down-regulated in the infected groups (Fig. 4B). After 72 h, 12 metabolites were up-regulated and 20 metabolites were down-regulated at the positive ion mode in the infected groups (Fig. 4A). While at the negative ion, 10 metabolites were up-regulated and 6 were down-regulated in the infected groups (Fig. 4B). The comparison between the uninfected groups at 24 h and 72 h post-infection showed that at positive ionization mode, 2 metabolites were up-regulated and 12 were down-regulated in 72 h-uninfected groups. While at negative ion, only 1 metabolite was up-regulated in the 72 h-uninfected. Furthermore, we performed a comparison between the infected groups at 24 h- and 72 h and found that a total of 25 up-regulated and 18 down-regulated metabolites in both positive and negative ionization modes. Whereby, at positive ionization mode 11 metabolites were up-regulated and 16 were down-regulated in the 72 h-infected groups at the positive ionization mode. While at the negative ion 14 metabolites were up-regulated and only 2 were down-regulated in the 72 h-infected groups (Fig. 4).

3.2. Differential enriched pathways analysis

We applied pathway enrichment analysis to differentiate pathways that participated in response to the *C. irritans* infection and found 66 pathways enriched with 164 compounds, 26 categories, and 66

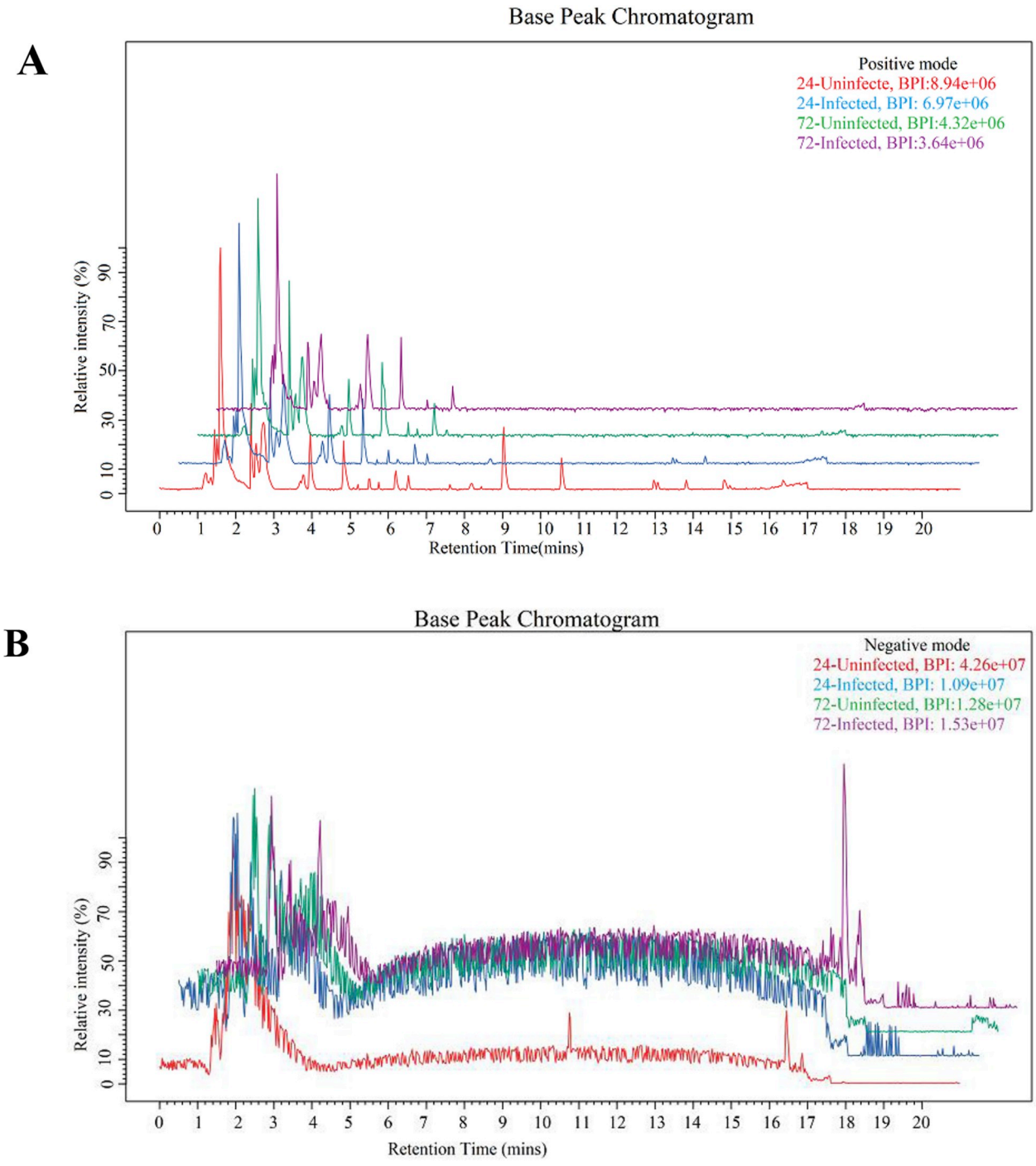

Fig. 1. Total ion chromatogram (TIC) for a typical sample, (A) for positive typical sample, (B) for negative typical sample.

subcategories (Table S1). When the compounds were analysed to remove duplicates we found 15 compounds namely cpd:C00025, cpd:C00042, cpd:C00049, cpd:C00079, cpd:C00122, cpd:C00127, cpd:C00147, cpd:C00149, cpd:C00158, cpd:C00262, cpd:C00300, cpd:C00366, cpd:C00414, cpd:C05953 and cpd:C14765 appeared repeatedly in the categories (Table S1). These include genetic information processing (1 category, 1 subcategory), metabolism (12 categories and 41 subcategories), cellular processes (1 category, 1 subcategory), environmental information processing (3 categories, 3 subcategories), organismal systems (5 categories, 12 subcategories), and human diseases (4 categories, 8 subcategories) (Table S1).The results showed further that the comparison between the infected and the uninfected groups at 24 h, in the differential enriched pathways included 25 categories and 58 subcategories (49 up, 9 down). Among these, 49 up-regulated subcategories in the top 10 include glutathione metabolism, gap junction, glutamatergic synapse, long-term depression, huntington's disease, alanine, aspartate and glutamate metabolism, biosynthesis of plant secondary metabolites, glyoxylate and dicarboxylate metabolism, histidine metabolism, and phenylalanine metabolism. While of the 9 down-regulated the top 6 in the pathways were tyrosine metabolism, synaptic vesicle cycle, taurine, and hypotaurine metabolism, taste transduction, two-component system, and toluene degradation (Table S1). The comparison between the infected and the uninfected group at 72 h involved 6 categories and 8 subcategories (4 up, 4 down). Among these, 4 up-regulated subcategories involved pathways such as GABAergic synapse, glutathione metabolism, zeatin biosynthesis, and

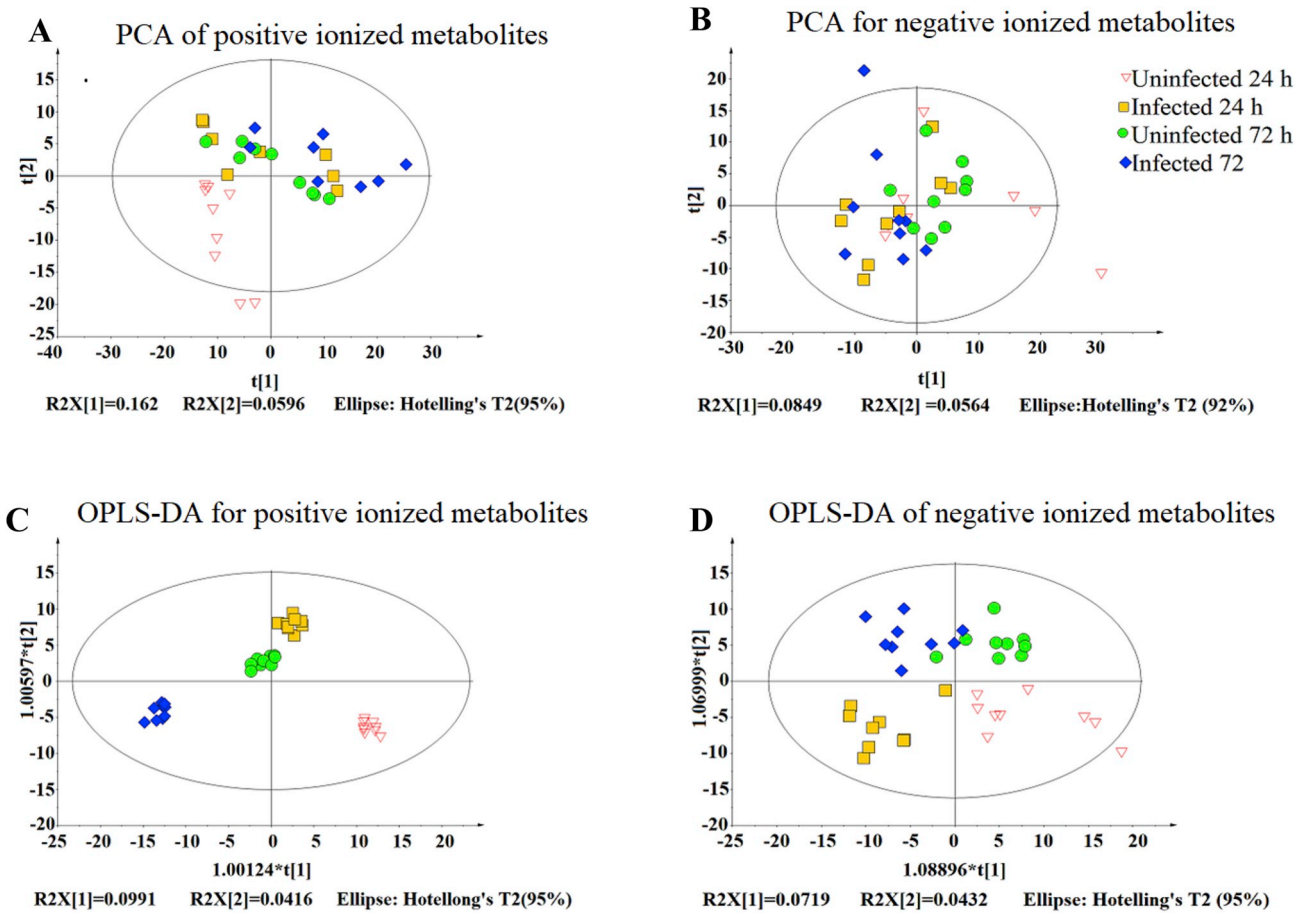

Fig. 2. The PCA and OPLS-DA score plots for a typical sample, showing the differences in the metabolite profiles among the groups. The abscissa is the score of the sample of the first principal component and the ordinate is the score of the sample of the second principal component. R2X [1] = 0.0991, the interpretability of the first principal component of the model; R2X [2] = 0.0416, the interpretability of the second principal component of the model (A) for PCA score plot positive mode (B) for PCA score plots negative mode (C) for OPLS-DA score plot positive mode and (D) for OPLS-DA score plot negative mode.

Table 1
OPLS-DA model validation parameters.

Groups	Principal fraction	R2X	R2Y	Q2
Treatment Vs Control 24 h V treatment Vs Control 72hrs (Positive)	3 + 3+0	0.354	0.976	0.6
Treatment Vs Control 24hrs(Positive)	1 + 1+0	0.257	0.963	0.637
Treatment Vs Control 72hrs(Positive)	1 + 3+0	0.388	1	0.709
Control 72 h V control 24hrs(Positive)	1 + 2+0	0.301	0.999	0.78
Treatment 72 h V Treatment 24hrs (Positive)	1 + 2+0	0.355	0.999	0.721
Treatment Vs Control 24 h V treatment Vs Control 72hrs(Negative)	3 + 0+0	0.154	0.822	0.186
Treatment Vs Control 24hrs(Negative)	1 + 4+0	0.367	1	0.501
Treatment Vs Control 72hrs(Negative)	1 + 4+0	0.367	1	0.382
Control 72 h V control 24hrs(Negative)	1 + 1+0	0.174	0.986	0.203
Treatment 72 h V Treatment 24hrs (Negative)	1 + 4+0	0.352	1	0.265

OPLS-DA model validation parameters, R2X: model (for X-variable datasets) interpretability; R2Y: model (for Y-variable datasets) interpretability; Q2: model predictability.

arachidonic acid metabolism. While the 4 down-regulated subcategories involved pathways including serotonergic synapse, purine metabolism, linoleic acid metabolism, and bile secretion (Table S1). On the other hand, the comparison between the uninfected at 72 h and the uninfected 24 h groups found 11 categories and 22 in subcategories (12up, 10 down). Among these, 12up-regulated subcategories in the top pathways included D-glutamine and D-glutamate metabolism, GABAergic synapse, glutathione metabolism, gap junction, glutamatergic synapse, long-term depression, and huntington's disease. Whereas, in the 10 down-regulated subcategories in the top five pathways were taurine and hypotaurine metabolism, taste transduction, retrograde endocannabinoid signalling, synaptic vesicle cycle, and C5-Branched dibasic acid metabolism(Table S1). Finally, the comparison between the infected 72 h V the infected 24 h groups revealed 13 categories and 35 in subcategories (10up, 25 down). Among these, 12up-regulated subcategories in the top pathways were biosynthesis of plant hormones, biosynthesis of plant secondary metabolites, glyoxylate and dicarboxylate metabolism, phenylalanine metabolism, degradation of aromatic compounds, methane metabolism, propanoate metabolism, chlorocyclohexane, and chlorobenzene degradation. Whereas in the 10 down-regulated subcategories involved pathways such as tyrosine metabolism, serotonergic synapse, renal cell carcinoma, styrene degradation, and metabolic pathways (Table S1). Based on the these results, most of the differential enriched pathways were mainly enriched in the metabolic pathway classes caused by carbohydrate metabolism, energy metabolism, lipid metabolism, nucleotide metabolism, metabolism of other amino acids, and amino acid metabolism as portrayed (Fig. 5). Therefore, we describe the variation of the metabolites in these pathways.

3.3. Identification of differential metabolite

Out of 2694 primary metabolites detected from both positive and negative ionization modes, only 23 metabolites could be clearly

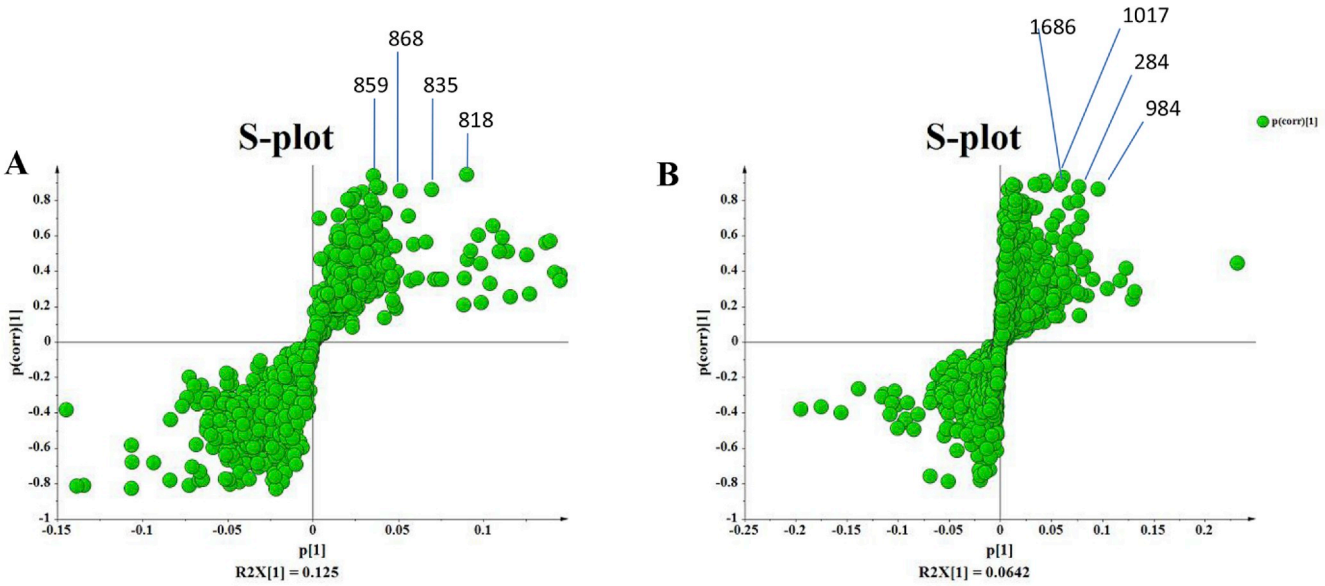

Fig. 3. S-plots provide visualization of OPLS-DA predicted principal component showing the screened out differential metabolites (biomarkers). The closer the metabolites to the lower left (left bottom) and upper right (top right) the greater the contribution they contributes to the differences between treatments.

identified and semiquantified with a known identification number. These metabolites were assigned into 66 KEGG pathways including metabolic pathways, biosynthesis of secondary metabolites, taurine, and hypotaurine metabolism, purine metabolism, linoleic acid metabolism, phenylalanine, tyrosine and tryptophan biosynthesis, glutathione metabolism, and alanine, aspartate, and glutamate metabolism. Additionally, out of the identified metabolites, only 6 were differentially expressed, namely 15-hydroxy- eicosatetraenoic acid (15-HETE), (S)-(−)-2-Hydroxyisocaproic acid, adenine, delta-valerolactam, betaine,and L-glutamate (Table 2).The KEGG analysis was assigned to different pathways and finally, the results were visualized in the heat maps of the differential hierarchical cluster analysis. Fig. 6 (A and B), shows the clustering of the infected and the uninfected groups with different metabolite regulation levels at a different time of infection. Each color in the heat map symbolizes the concentration of the given metabolite in the skin samples based on the normalized signal intensities. A comprehensible separation of the infected and the uninfected groups, as reported in this study, is a strong sign of the difference

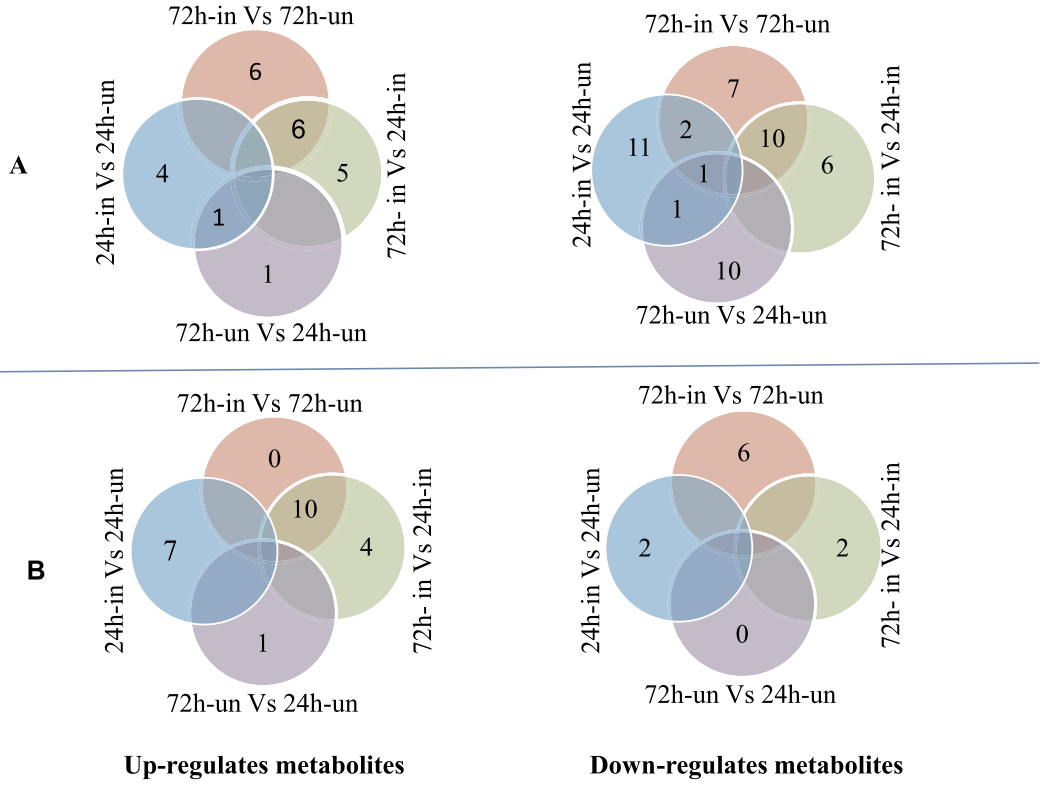

Fig. 4. Number of up and down-regulated metabolites for positive (A) and negative (B) ionization modes. Comparison of differences metabolism Venn diagram displays down and up-regulation in metabolite. In each circle, the number represents the number of differential metabolites intersected by the alignment group. (24 h-un for 24 h-uninfected, 24 h-in for 24 h-infected, 72 h-un for 72 h-uninfected and 72 h-in for 72 h-infected).

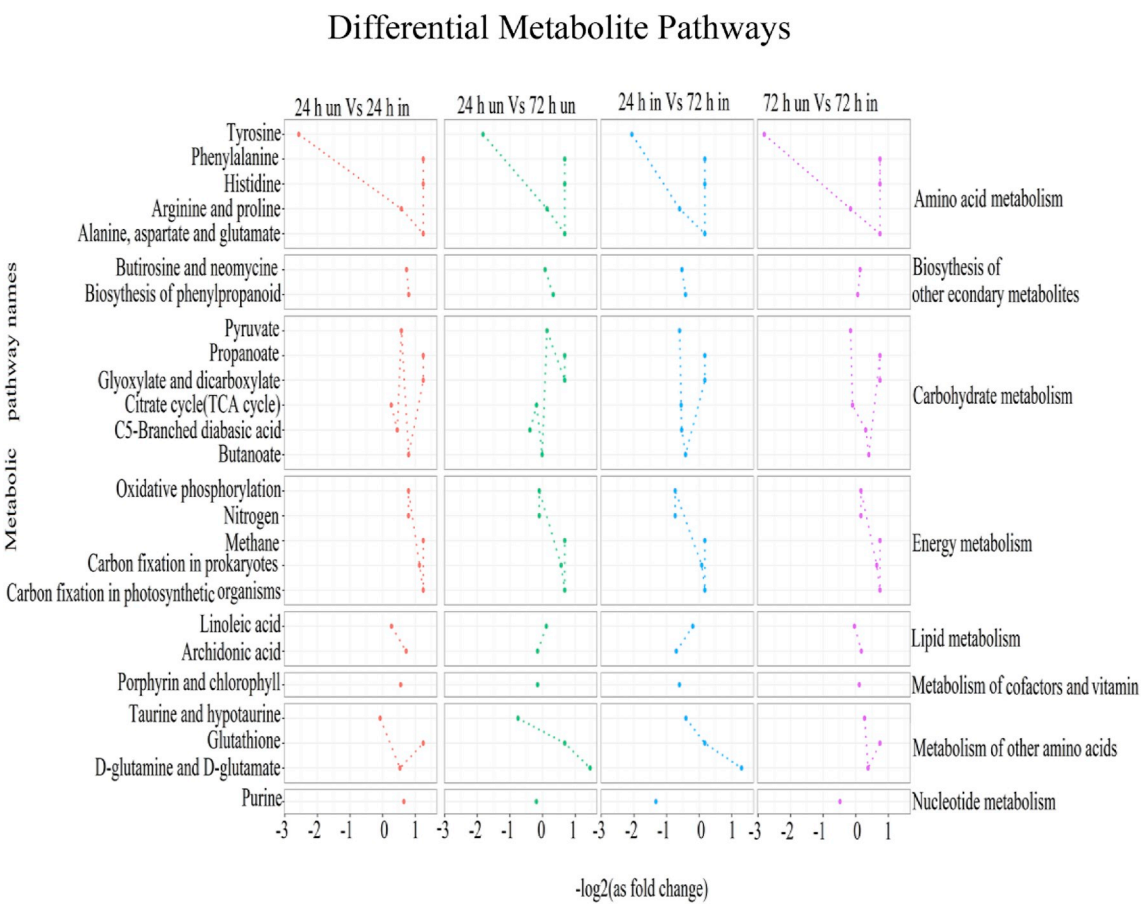

Fig. 5. Different groups of metabolic pathway heat maps, where the Pathway Activity Profiling (PAPi) algorithm is used to calculate the activity score (AS) for each metabolic pathway based on the number and relative abundance of each metabolic pathway in the KEGG database degree. The upper panel is based on metabolic processes and is categorized. The dot pattern of the above metabolic pathways is statistically tested for the KEGG metabolic pathway (ANOVA p-value < 0.05).

in metabolites expressed involving the two groups. Furthermore, categorization of the detected metabolites in response to *C. irritans* infection was done and revealed different kinds of metabolites significantly altered abundances at $P < 0.05$ as follows.

Acomparison of amino acids metabolites (L-phenylalanine, glutathione oxidized, L-glutamate, creatine, L-valine, (S)-(−)-2-Hydroxyisocaproic acid, and L-aspartic acid) at 24 h exposure to *C. irritants*, showed a significant down-regulated concentration of L-glutamate, while there were no significant differences in other metabolites. At 72 h, (S)-(−)-2-Hydroxyisocaproic acid, was significantly up-regulated in the 72 h infected group. Whereas, the comparison between the 72 h-uninfected and the 24 h-uninfected groups as well as the 72 h-infected and the 24 h-infected groups, did not reveal any significant differences among the groups (Fig. 7). When the groups were compared for organic acid (fumaric acid, malic acid, citric acid, succinic acid, uric acid and 15-HETE), 15-HETE was significantly up-regulated in the 72 h infected group while other metabolites had no significant differences among the groups (Fig. 8). On the other hand, when the groups were compared for osmolyte metabolites (betaine, taurine, and glycerophosphocholine), the results showed that betaine was significantly down-regulated in the 72 h infected group, while other metabolites had no significant differences among the groups (Fig. 9). Furthermore, the comparison for nucleosides and derives (guanine and hypoxanthine and adenine) showed that adenine was significantly up-regulated at the 72 h while other metabolites had no significant differences among the groups (Fig. 10). Another metabolite, which was found to be significantly up-regulated in the 24 h infected group, was delta-Valerolactam (Table 2).

3.4. Metabolites associated network analysis

Fig. 11 shows the correlation network analysis between metabolites and metabolites, which was performed using R (v3.1.3) at the absolute value of the correlation coefficient $R \geq 0.7$ & FDR p-value ≤ 0.05. It displays networks, which were generated by correlation-based network analysis of the sets of data profiles from the fish skin. At 24 h post infection, the connectivity between 3-Buten-1-amine and 13-OxoODE, as well as citric acid and hypoxanthine showed a negative association, while connectivity of all metabolites showed a positive association at 72 h post-infection.

4. Discussion

The study of metabolomics has been used to show alteration in metabolites which are essential for several metabolic pathways in different fish species organs include skin mucus, liver, and kidney [33,36,37]. Nevertheless, metabolic variations in the skin of *N. albiflora* during *C.irritans* infections have until now been elusive. Using an LC-MS metabolomic approach, we observed metabolic responses reflected in the skin of *N. albiflora* during 24 h and 72 h post-infection with *C.irritans*. Therefore, in the current paper, we discuss the functional significance of the skin metabolome, specifically the more abundant metabolites putatively annotated and their potential functions in skin innate immune system.

4.1. Skin metabolome changes and their physiologic significances

Metabolites are essential marks of metabolic pathways and mechanisms such as inflammation, disruptions of tricarboxylic acid (TCA)

Table 2
Metabolites obtained data matrices at both positive [M + H] + negative [M-H]-ion mode.

Type	Metabolite	KEGG	Infected Vs uninfected at 24 h Folds	Infected Vs uninfected at 72 h Folds	Uninfected 72 h Vs uninfected 24 h Folds	Infected 72 h Vs infected 24 h Folds
[M+H]+	2-Aminopropanol	NA	-0.19	-0.10	0.29	0.37
[M+H]+	3-Buten-1-amine	C12244	-0.01	0.96	-0.41	0.57
[M+H]+	Acetylcholine	C01996	-0.89	0.50	-0.84	0.55
[M+H]+	L-Valine	C00183	0.39	0.37	0.62	0.60
[M+H]+	L-Glutamate	C00025	-1.25	-0.74	-0.68	-0.18
[M+H]+	Guanine	C00242	0.95	-0.56	1.24	-0.27
[M+H]+	Taurine	C00245	-0.41	-1.00	0.04	-0.55
[M+H]+	Glycerophosphocholine	NA	-1.25	-2.31	0.32	-0.74
[M+H]+	delta-Valerolactam	NA	-0.52	-1.62	0.59	-0.52
[M+H]+	Butanone	C02845	-0.11	-0.89	-0.87	-1.65
[M+H]+	Cyclohexanone	C00414	-0.54	-0.38	-1.46	-1.30
[M+H]+	Betaine	C00719	0.13	-1.09	0.36	-0.86
[M-H]-	15-HETE	NA	0.79	2.14	0.85	2.20
[M-H]-	(S)-(-)-2-Hydroxyisocaproic acid	NA	-0.86	2.35	-0.46	2.75
[M-H]-	Adenine	C00147	-0.25	1.68	-0.03	1.90
[M-H]-	13-OxoODE	C14765	0.94	2.38	0.56	2.00
[M-H]-	PGA2	C05953	2.57	2.80	1.83	2.06
[M-H]-	Citric acid	C00158	-1.11	-0.23	0.09	0.97
[M-H]-	(S)-2-Hydroxyglutarate	C03196	-0.46	0.14	0.29	0.89
[M-H]-	Malic acid	C00149	-0.60	-0.32	0.29	0.58
[M-H]-	L-Phenylalanine	C00079	-0.65	0.48	0.19	1.32
[M-H]-	Fumaric acid	C00122	-0.46	0.36	-0.18	0.64
[M-H]-	Succinic acid	C00042	-0.74	-0.14	-0.08	0.53
[M-H]-	Glutathione, oxidized	C00127	-0.31	-0.21	0.24	0.34
[M-H]-	L-Aspartic Acid	C00049	0.07	-0.27	0.75	0.40
[M-H]-	Uric acid	C00366	0.26	0.37	-0.05	0.06
[M-H]-	Hypoxanthine	C00262	0.61	0.74	-0.17	-0.04
[M-H]-	Creatine	C00300	0.67	0.59	-0.09	-0.16

The fold change was calculated using a formula log2 (Infected/uninfected). Bold and red represents significant upregulated value, ($P < 0.05$). Underlined and green stands for decreased significantly ($P < 0.05$).

cycle, metabolism amino acid, protein synthesis, and oxidative phosphorylation which are related to the natural immune response during infection [38]. Previous research findings on *N. albiflora* challenged with *C. irritans* revealed that the infected fish resumed feeding after 72 h [5]. The studies reveal further that *N. albiflora* could not die off in the culture system when they are infected with *C. irritans* at a median lethal concentration (2050 theronts/g fish) for up to 15 days and the pathogens vanished progressively [5]. Our study revealed that the number of differential enriched pathways were higher in 24 h group with 22 categories and 58 subcategories (49 up, 9 down) while at 72 h the differential enriched pathways were 6 categories and 8 subcategories (4 up, 4 down). However, it is well known that to survive with a lethal infection, fish have the biological needs such as continuously secretion and replacing mucus layer [39], energy metabolism [40] immunological responses [41], as well as functioning osmoregulatory and respiratory systems [42]. Most of the differential enriched pathways were mainly from metabolic pathway classes which may be associated with the elevation of immune protection [43] (although not directly involved) including glutathione metabolism [44], taurine and hypotaurine metabolism [45], purine metabolism [46], arachidonic acid metabolism [47], oxidative phosphorylation [48], TCA cycle [49] and histidine metabolism [50]. Therefore, the higher number of differential enriched pathways, which were found at 24 h as opposed to that at the 72 h, may signify that the *C. irritans* caused a strong metabolic stress on the *N. albiflora* at 24 h of infection. Furthermore, the restoration of the dysregulated metabolic state could take place at 72 h to recover the normal healthy state of the *N. albiflora.* This result is as well supported by the PCA plot analysis, whereby at 24 h there were much differences between infected and uninfected (separately clustered) while at 72 h there were no much difference between infected and uninfected. These results are also consistent with the findings from previous studies that reported the recovering of feed intake and repository rate in the infected *N. albiflora* [5] and regulation of more miRNA involved in regulating body restoration and immune depression at 72 h [6].

4.2. Immunological responses to C. irritans infection

Parasite infections stimulate inflammation and change of the structure and function of the infected tissues [51]. Furthermore, the parasitic infection causes fish to flash (scratch), unusual swimming, sluggish or taking breaths more quickly as if in pain [3] just like convulsion in other animals. Other researchers have verified that *C. irritans* infection causes an acute phase of inflammation [52], which has been reported to cause convulsion/seizures in the infected fish and mice [53,54]. According to Sharkey, the inflammation comprises of different series of homeostatic mechanisms involving the immune, nervous, and circulatory systems in response to infection [55]. It initiates the killing of pathogens and involves the process of tissue repair so as to help in bringing back of homeostasis at diseased or injured sites by secreting anti-inflammatory cytokines, and activating regulatory cells [56,57].

15-HETE is the metabolites of 15-Lipoxygenases, which are synthesized by various cells including macrophages and neutrophil that exhibit anti-inflammatory and immunomodulatory properties [58]. Also, adenine nucleotides are regarded as vital endogenous signaling molecules in inflammatory and immunological responses [59,60] and an important component in the purinergic system in the regulation of immune and inflammatory responses in the fish plasma membrane [61,62]. Numerous reports have suggested that the purinergic cascade plays a significant role in regulating inflammatory and immune

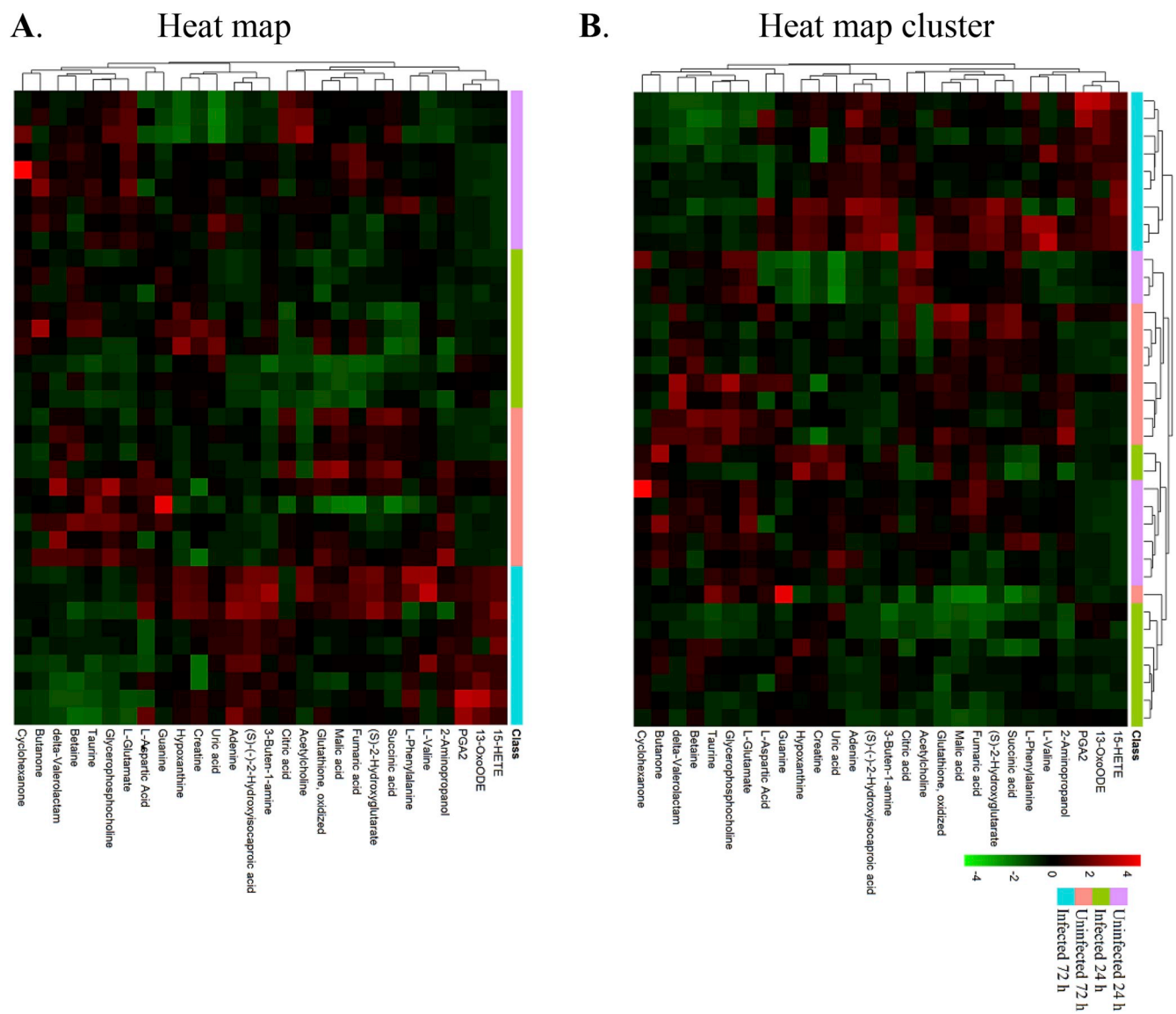

Fig. 6. Heat map showing the metabolites detected. Red and Green indicate an increase and decrease of metabolites relative to the median metabolite level, respectively (see color scale). (For interpretation of the references to color in this figure legend, the reader is referred to the Web version of this article.)

responses during diseases, in attempting to weaken inflammatory tissue damage [63]. In our study, we found no significant changes at 24 h in the levels of 15-HETE and adenine while at 72 h, post-infection levels were significantly increased in the infected group as opposed to the uninfected group. The increase in 15-HETE found in this study is consistent with the finding earlier reported in vitro which revealed that the exposure of macrophages to *Toxoplasma gondii* activates an up-regulation in arachidonic acid release and lipoxygenase activity that largely favours the production of 12-HETE [64]. Similarly, it was previously reported that during the chronic infection, the production of 15-HETE increases in mice infected with an intracellular parasitic protozoan *T. gondii* [65]. Furthermore, the observed up-regulation in adenine in this study would produce adenosine [66,67], which is responsible for the anti-inflammatory and for the reduction of skin damage. In addition, this result is in agreement with previous results reported during *Streptococcus agalactiae* infection in silver catfish [62]. Therefore, the reported up-regulationin adenine could increase the amount of ATP, which is the main detector of inflammation [68]in the skin tissue of the infected fish. On the other hand,15-HETE could be involved in regulating inflammation as well as other responses such as hindering the production of or actions of the pro-inflammatory eoxins, which in turn, can be suggested as an anti-inflammatory in response to the infection.

Betaine is a lipotropic compound that catalyses the metabolism of lipid in animals [69] and improves energy metabolism through the production of carnitine, which transports long-chain fatty acids to the mitochondria for oxidation [70]. Furthermore, betaine has been identified as having an immunostimulatory function in fish [71] due to their role in DNA methylation which takes place during the identification of immune and production of antibody [72]. Previously, Klasing *et al.* [73] verified that betaine has an effect on the pathogenesis of *Eimeria acervulina* infection in chicks through enhancing phagocytosis of *E. acervulina* by macrophages and NO release from heterophils and macrophages which are critical effectors function in defence against parasites [74]. In their study, they also recognized the modulatory effect of betaine to the development of monocyte chemotaxis and nitrous oxide production by heterophils and macrophages. Moreover, a dietary betaine supplementation was reported to improve growth performance and survival rate in common carp *Cyprinus carpio* [75]. Previous study on clam *R. Philippinarum* which were infected with *V. anguillarum,V. splendidus* and *V. harveyi* [27,28] showed up-regulation of betaine in the infected groups, in our current study on the other hand, there was a significant decline in the level of betaine in the infected fish at 72 h

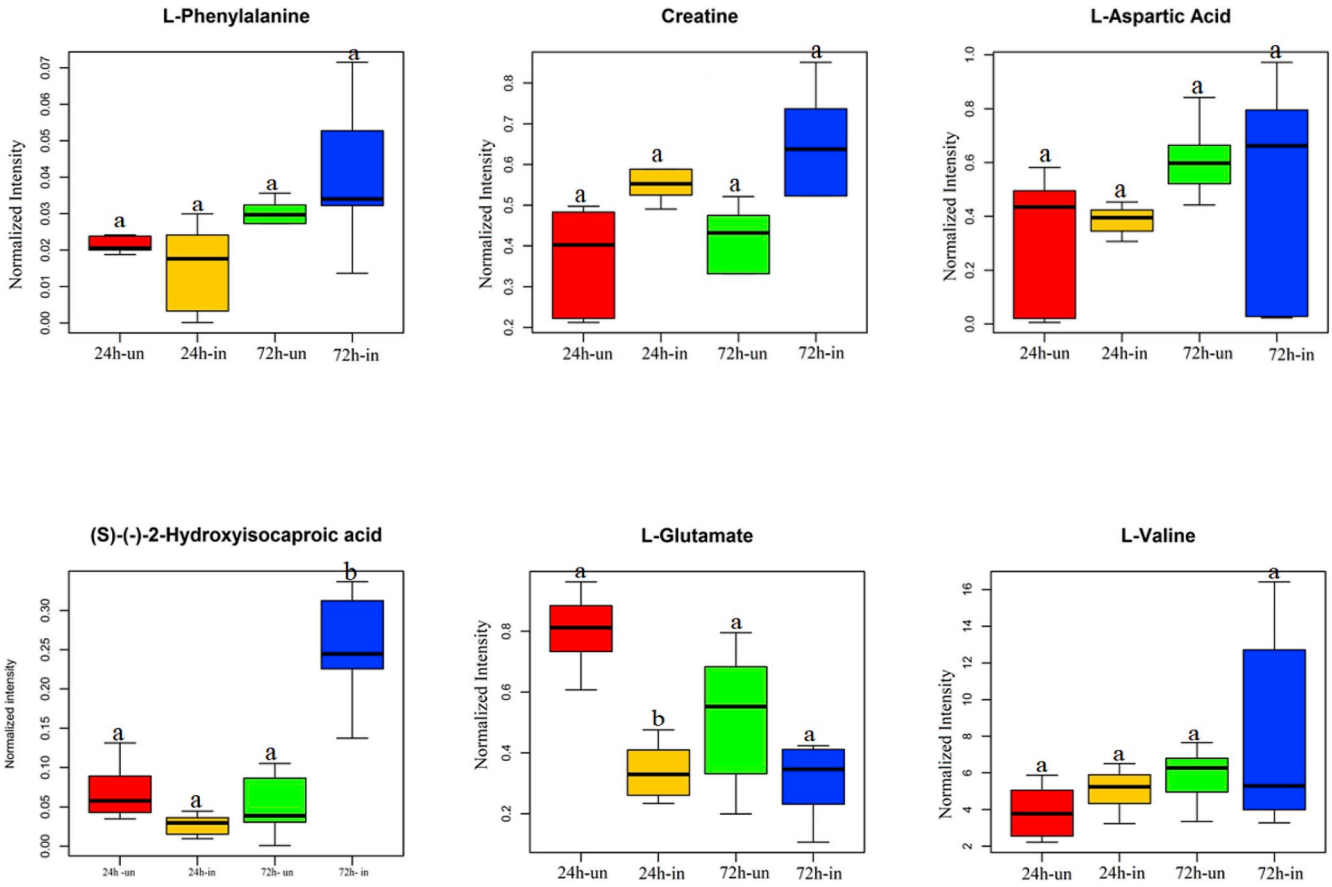

Fig. 7. Box diagram analysis, the difference in amino acids, metabolites between the infected and uninfected groups at a different time of infection at $P < 0.05$. (24 h-un for 24 h-uninfected, 24 h-in for 24 h-infected, 72 h-un for 72 h-uninfected and 72 h-in for 72 h-infected). Latter b shows statistical significant.

postinfection. However, it has been reported that *C. irritans* infection causes an osmotic imbalance due to damage in the gill chloride cells which are mainly hindered by the discharge of ions [41] because of the dehydration associated with the infection. Therefore, one would suppose that there would be an accumulation of more betaine in the infected fish than in the uninfected in an effort to maintain a normal osmotic balance. On the contrary, our analysis shows that the infection with *C. irritans* caused down-regulation of betaine at 72 h post-infection. This is because the infections caused skin lesions and, as a result, the decreases are probably due to, in part, the impaired abortion. This could compensate increases of the amounts of betaine, which may have been accumulated in response to the hyperosmotic extracellular conditions [76].

4.3. Identified biomarkers

Biomarkers are biological molecules which indicate normal or abnormal process occurring in the body, responsible for metabolic attributes, and disclosing metabolic mechanisms during infections [18]. These biomarkers can be used in pinpointing of elevated incidence of disease and pathological conditions in aquatic organisms [77,78]. In our analysis during 72 h post infection a total of 17 compounds (8 at positive ionization mode and 9 at negative ionization mode) were identified as biomarkers by screening out the differential metabolites with high s-plot, P-value and P corr. Though we could not identify the names of the obtained biomarkers, at present we can use them in the diagnosis and management of *C. irritans* infection. Moreover, we will be able to link these biomarkers with their biological mechanisms in the near future once we know exactly the metabolites represented by these biomarkers.

4.4. Energy metabolism in response to C. irritans infection

Health status and physiological processes of the organism's body are determined by an alteration in the number of metabolites. When fish are infected by *C. irritans* their feeding rate drops suddenly which is also regarded as a precursor for many fish deaths [7]. The study by Ellis *et al.* (2014) suggested that exposure to *V. tubiashii* infection is energetically costly [79]. Studies on sea bream *P. major*, tiger puffer *Takifugu rubripes*, and marbled rockfish *Sebastiscus marmoratus* show that when they get infected by *C. irritans,* they die on the second or third day after the drop of feeding rate [80,81]. However, to overcome the stresses caused by the pathogen, the infected fish needs to consume large amounts of energy [7,8,81]. Metabolism of amino acids is very essential for energy dissipation, synthesis of protein for the purpose of detoxification and fundamental organic molecules for safekeeping innate immune responses in fish [29,82]. L-glutamate is a non-essential amino acid important in anaplerotic reactions in the TCA cycle and function as a signalling means connecting the immune and nervous systems [83–85]. Furthermore, L-glutamate is a key in a pathway process of biochemical degradation, and a precursor for other amino acids including glutathione, which is important in preventing oxidative

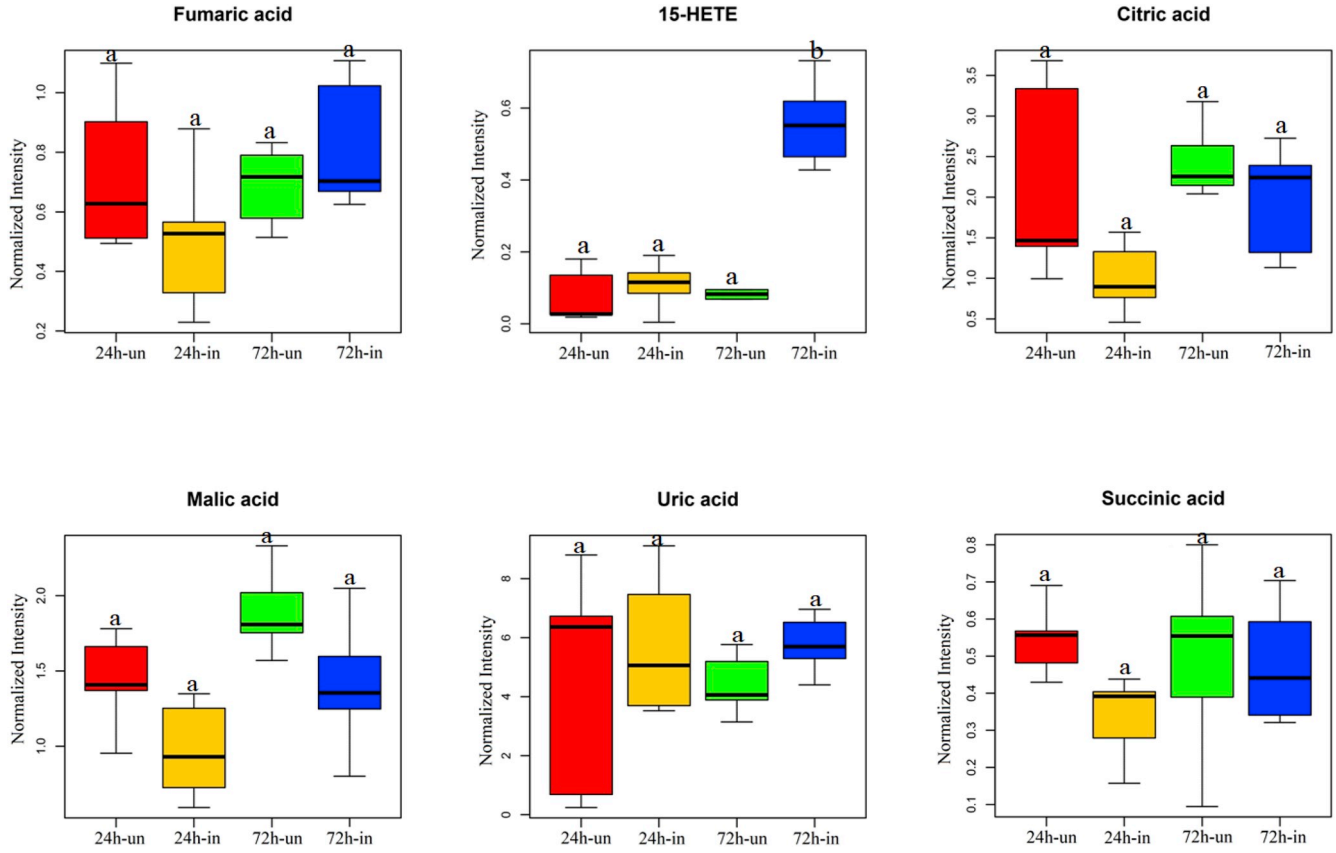

Fig. 8. Organic acid metabolites between the infected and uninfected groups at a different time of infection at P < 0.05. (24 h-un for 24 h-uninfected, 24 h-in for 24 h-infected, 72 h-un for 72 h-uninfected and 72 h-in for 72 h-infected). Latter b shows statistical significant.

injury [86,87]. In our study, the down-regulation in L-glutamate at 24 h might be caused by the immediately energy demand for maintenance of the immune response to control *C. irritans* infection, which led to the active energy generation by TCA cycle using L-glutamate. This is done to overcome the detrimental effects caused by pathogens and boost up the immune system [88].

5. Conclusion

We reported a strong relationship between skin metabolome of *N. albiflora* and *C. irritans* infection. Different major perturbations on the innate immune system of the *N. albiflora* resulting from *C. irritans* infection have been established, including inflammation, disruption of TCA cycle, and changes in amino acid metabolism. Also, a total of 17 compounds have been identified as potential biomarkers. Considerable changes in different metabolites have been identified. Among them, L-glutamate, adenine, betaine, and 15-hydroxy-eicosatetraenoic acid (15-HETE) were involved in diverse metabolic, innate immune responses, and physiological roles and these could potentially be considered as biomarkers of *C. irritans* infection in *N. albiflora*. Our results therefore, further advance our understanding on the immunological regulation of *N. albiflora* during immune response against *C. irritans* infections.

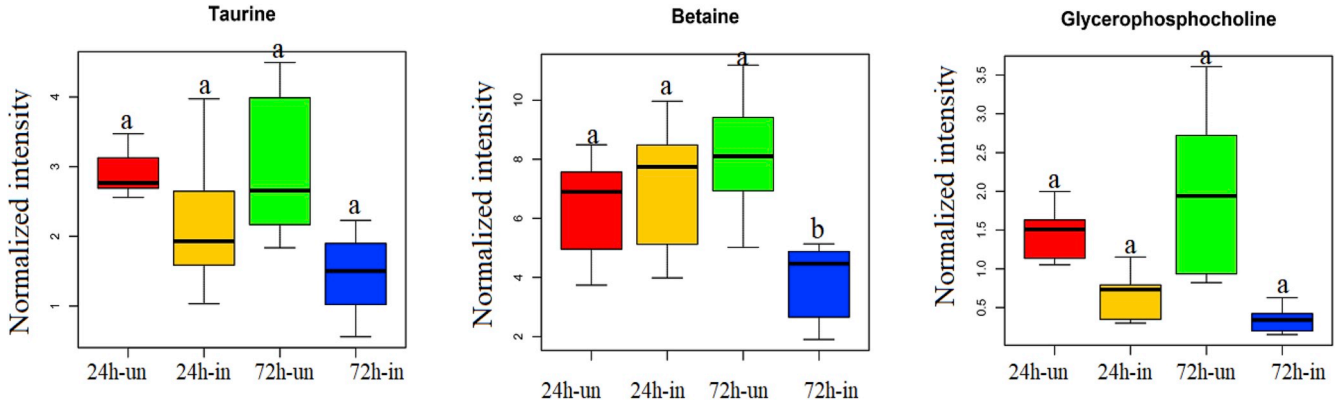

Fig. 9. Osmolytes metabolites between the infected and uninfected groups at a different time of infection at P < 0.05. (24 h-un for 24 h-uninfected, 24 h-in for 24 h-infected, 72 h-un for 72 h-uninfected and 72 h-in for 72 h-infected). Latter b shows statistical significant.

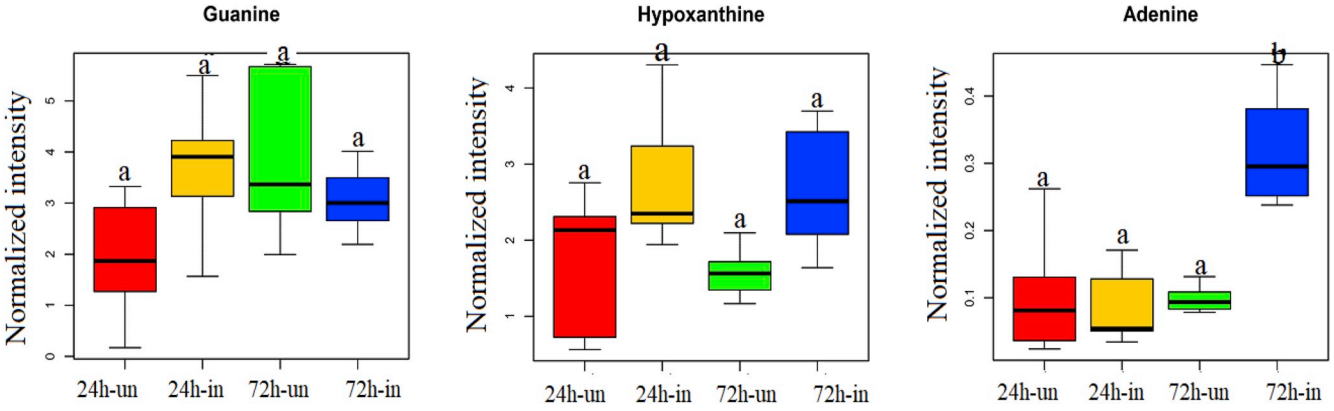

Fig. 10. Nucleosides and derives between the infected and uninfected groups at a different time of infection at $P < 0.05$. (24 h-un for 24 h-uninfected, 24 h-in for 24 h-infected, 72 h-un for 72 h-uninfected and 72 h-in for 72 h-infected). Latter b shows statistical significant.

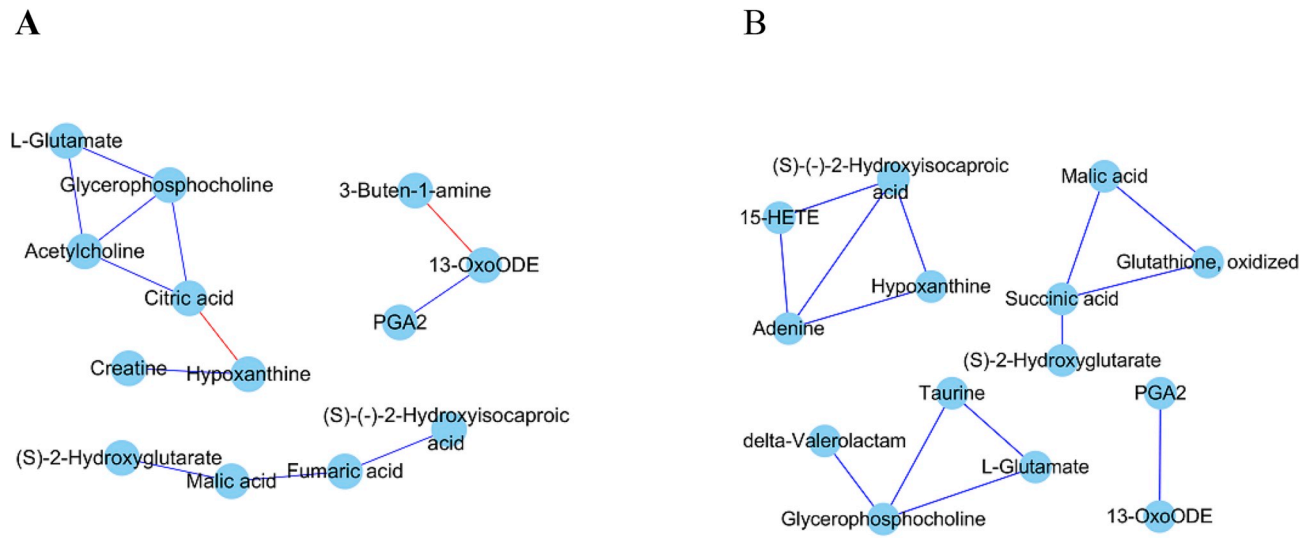

Fig. 11. Metabolite association network analysis showing the correlation analysis between metabolites and metabolites. A for 24 h postinfection, and B for 72 h postinfection, red lines connectivity shows a negative association and blue lines connectivity showed a positive association between metabolites. (For interpretation of the references to color in this figure legend, the reader is referred to the Web version of this article.)

Acknowledgments

This work was funded by the Zhejiang Provincial Natural Science Foundation (grant no. LY18C190005); the Ningbo University Research Start-Up Fund for the Backbone of Scientific Research (grant no. 421707390); Ningbo University Research Start-Up Fund for excellent PhD (013-421807990, 013-421906192); and the K. C. Wong Magna Fund in Ningbo University.

Appendix A. Supplementary data

Supplementary data to this article can be found online at https://doi.org/10.1016/j.fsi.2019.09.027.

Author contributions

Ivon F. Maha, Xiao Xie, Fei Yin, and Dong Qian conceived and designed the study. Suming Zhou, Youbin Yu, Xiao Liu, Aysha Zahid, Yuhua Lei, Rongrong Ma performed both animal feeding and laboratory experiments, analysed the sequencing data, interpreted the data, and prepared figures and tables. Ivon F. Maha and Xiao Xie wrote the manuscript. Ivon F. Maha, Xiao Xie, and Fei Yin interpreted the data, wrote, and revised the paper. All authors read and approved the final manuscript.

Compliance with ethical standards

All animal and parasite experiments were performed according to local and central government regulations. All experiments were approved by the Institutional Animal Care and Use Committee of the Ningbo University.

Declarations of interest

None.

References

[1] A.G. Swennes, J.G. Noe, R.C. Findly, H.W. Dickerson, Differences in virulence between two serotypes of *Ichthyophthirius multifiliis*, Dis. Aquat. Org. 69 (2006) 227–232.
[2] R. Yanong, *Cryptocaryon irritans infections* (marine white spot disease), Fish. Progr Fish Aquat Sci SFRC, Florida Coop Exten - sion Serv Inst Food Agric Sci Univ Florida, Gainesville, FL, 2009, pp. 1–9.
[3] A. Colorni, P. Burgess, *Cryptocaryon irritans* Brown 1951, the cause of “white spot disease” in marine fish: an update, Aquarium Sci. Conserv. 1 (1997) 217–238.
[4] F. Yin, W. Liu, P. Bao, S. Jin, D. Qian, J. Wang, et al., Comparison of the susceptibility and resistance of four marine perciform fishes to *Cryptocaryon irritans* infection, Fish Shellfish Immunol. 77 (2018) 298–303.
[5] F. Yin, W. Liu, P. Bao, B. Tang, Food intake, survival, and immunity of *Nibea albiflora* to *Cryptocaryon irritans* infection, Parasitol. Res. 117 (2018) 2379–2384.
[6] X. Xie, R. Ma, D. Qian, Y. Yu, X. Liu, Y. Lei, et al., microRNA regulation during *Nibea*

albiflora immuno-resistant against *Cryptocaryon irritans* challenge in fish skin, Aquaculture 507 (2019) 211–221.
[7] F. Yin, H. Gong, Q. Ke, A. Li, Stress, antioxidant defence and mucosal immune responses of the large yellow croaker *Pseudosciaena crocea* challenged with *Cryptocaryon irritans*, Fish Shellfish Immunol. 47 (2015) 344–351.
[8] F. Yin, X.M. Dan, P. Sun, Z.H. Shi, Q.X. Gao, S.M. Peng, et al., Growth, feed intake and immune responses of orange-spotted grouper (*Epinephelus coioides*) exposed to low infectious doses of ectoparasite (*Cryptocaryon irritans)*, Fish Shellfish Immunol. 36 (2014) 291–298.
[9] Y. Li, Q. Xiang, Q. Zhang, Y. Huang, Z. Su, Overview on the recent study of antimicrobial peptides: origins, functions, relative mechanisms and application, Peptides 37 (2012) 207–215.
[10] E.M. Ángeles, An overview of the immunological defenses in fish skin, ISRN Immunol. (2012) 1–29 2012.
[11] Y. Hu, A. Li, Y. Xu, B. Jiang, G. Lu, X. Luo, Transcriptomic variation of locally-infected skin of *Epinephelus coioides* reveals the mucosal immune mechanism against *Cryptocaryon irritans*, Fish Shellfish Immunol. 66 (2017) 398–410.
[12] D.S. Kelkar, E. Provost, R. Chaerkady, B. Muthusamy, S.S. Manda, T. Subbannayya, et al., Annotation of the zebrafish genome through an integrated transcriptomic and proteomic analysis, Mol. Cell. Proteom. : MCP 13 (2014) 3184–3198.
[13] H. Ye, Q. Lin, H. Luo, Applications of transcriptomics and proteomics in understanding fish immunity, Fish Shellfish Immunol. 77 (2018) 319–327.
[14] J. Petit, L. David, R. Dirks, G.F. Wiegertjes, Genomic and transcriptomic approaches to study immunology in cyprinids: what is next? Dev. Comp. Immunol. 75 (2017) 48–62.
[15] L. Song, J. Zhang, C. Li, J. Yao, C. Jiang, Y. Li, et al., Genome-wide identification of Hsp70 genes in channel catfish and their regulated expression after bacterial infection, PLoS One 9 (2014) e115752.
[16] J. Cheng, W. Lan, G. Zheng, X. Gao, Metabolomics: a high-throughput platform for metabolite profile exploration, Methods Mol. Biol. 1754 (2018) 265–292.
[17] M. Reverter, P. Sasal, B. Banaigs, D. Lecchini, G. Lecellier, N. Tapissier-Bontemps, Fish mucus metabolome reveals fish life-history traits, Coral Reefs 36 (2017) 463–475.
[18] X.H. Chen, S.R. Liu, B. Peng, D. Li, Z.X. Cheng, J.X. Zhu, et al., Exogenous l-valine promotes phagocytosis to kill multidrug-resistant bacterial pathogens, Front. Immunol. 8 (2017) 207.
[19] B. Peng, H. Li, X.X. Peng, Functional metabolomics: from biomarker discovery to metabolome reprogramming, Protein & cell 6 (2015) 628–637.
[20] J. Zhang, H. Shen, W. Xu, Y. Xia, D.B. Barr, X. Mu, et al., Urinary metabolomics revealed arsenic internal dose-related metabolic alterations: a proof-of-concept study in a Chinese male cohort, Environ. Sci. Technol. 48 (2014) 12265–12274.
[21] K. Buchmann, T. Lindenstrom, Interactions between monogenean parasites and their fish hosts, Int. J. Parasitol. 32 (2002) 309–319.
[22] E. Kakazu, N. Kanno, Y. Ueno, T. Shimosegawa, Extracellular branched-chain amino acids, especially valine, regulate maturation and function of monocyte-derived dendritic cells, J. Immunol. 179 (2007) 7137–7146.
[23] H. Wu, C. Ji, L. Wei, J. Zhao, H. Lu, Proteomic and metabolomic responses in hepatopancreas of *Mytilus galloprovincialis* challenged by *Micrococcus luteus* and *Vibrio anguillarum*, J. Proteom. 94 (2013) 54–67.
[24] H. Zhang, L. Ding, X. Fang, Z. Shi, Y. Zhang, H. Chen, et al., Biological responses to perfluorododecanoic acid exposure in rat kidneys as determined by integrated proteomic and metabonomic studies, PLoS One 6 (2011) e20862.
[25] M. Jiang, Q.Y. Gong, S.S. Lai, Z.X. Cheng, Z.G. Chen, J. Zheng, et al., Phenylalanine enhances innate immune response to clear ceftazidime-resistant Vibrio alginolyticus in Danio rerio, Fish Shellfish Immunol. 84 (2019) 912–919.
[26] P.F. Liu, Q.H. Liu, Y. Wu, H. Jie, A pilot metabolic profiling study in hepatopancreas of *Litopenaeus vannamei* with white spot syndrome virus based on (1)H NMR spectroscopy, J. Invertebr. Pathol. 124 (2015) 51–56.
[27] X. Liu, C. Ji, J. Zhao, H. Wu, Differential metabolic responses of clam *Ruditapes philippinarum* to *Vibrio anguillarum* and *Vibrio splendidus* challenges, Fish Shellfish Immunol. 35 (2013) 2001–2007.
[28] X. Liu, J. Zhao, H. Wu, Q. Wang, Metabolomic analysis revealed the differential responses in two pedigrees of clam *Ruditapes philippinarum* towards *Vibrio harveyi* challenge, Fish Shellfish Immunol. 35 (2013) 1969–1975.
[29] J. Lu, Y. Shi, S. Cai, J. Feng, Metabolic responses of *Haliotis diversicolor* to *Vibrio parahaemolyticus* infection, Fish Shellfish Immunol. 60 (2017) 265–274.
[30] Z.X. Cheng, Y.M. Ma, H. Li, X.X. Peng, N-acetylglucosamine enhances survival ability of tilapias infected by Streptococcus iniae, Fish Shellfish Immunol. 40 (2014) 524–530.
[31] X.M. Dan, A.X. Li, X.T. Lin, N. Teng, X.Q. Zhu, A standardized method to propagate *Cryptocaryon irritans* on a susceptible host pompano *Trachinotus ovatus*, Aquaculture 258 (2006) 127–133.
[32] H. Wu, A.D. Southam, A. Hines, M.R. Viant, High-throughput tissue extraction protocol for NMR- and MS-based metabolomics, Anal. Biochem. 372 (2008) 204–212.
[33] D.R. Ekman, D.M. Skelton, J.M. Davis, D.L. Villeneuve, J.E. Cavallin, A. Schroeder, et al., Metabolite profiling of fish skin mucus: a novel approach for minimally-invasive environmental exposure monitoring and surveillance, Environ. Sci. Technol. 49 (2015) 3091–3100.
[34] R.B. Sotto, C.D. Medriano, Y. Cho, H. Kim, I.Y. Chung, K.S. Seok, et al., Sub-lethal pharmaceutical hazard tracking in adult zebrafish using untargeted LC-MS environmental metabolomics, J. Hazard Mater. 339 (2017) 63–72.
[35] Y. Ni, M. Su, J. Lin, X. Wang, Y. Qiu, A. Zhao, et al., Metabolic profiling reveals disorder of amino acid metabolism in four brain regions from a rat model of chronic unpredictable mild stress, FEBS Lett. 582 (2008) 2627–2636.
[36] B. Peng, Y.M. Ma, J.Y. Zhang, H. Li, Metabolome strategy against *Edwardsiella tarda* infection through glucose-enhanced metabolic modulation in tilapias, Fish Shellfish Immunol. 45 (2015) 869–876.
[37] P.F. Liu, Y. Du, L. Meng, X. Li, Y. Liu, Metabolic profiling in kidneys of Atlantic salmon infected with Aeromonas salmonicida based on (1)H NMR, Fish Shellfish Immunol. 58 (2016) 292–301.
[38] T.V. Nguyen, A.C. Alfaro, T. Young, S. Ravi, F. Merien, Metabolomics study of immune responses of New Zealand greenshell mussels (*Perna canaliculus*) infected with pathogenic *Vibrio sp*, Mar. Biotechnol. 20 (2018) 396–409.
[39] S. Benhamed, F.A. Guardiola, M. Mars, M.A. Esteban, Pathogen bacteria adhesion to skin mucus of fishes, Vet. Microbiol. 171 (2014) 1–12.
[40] L. Fernandez-Alacid, I. Sanahuja, B. Ordonez-Grande, S. Sanchez-Nuno, G. Viscor, E. Gisbert, et al., Skin mucus metabolites in response to physiological challenges: a valuable non-invasive method to study teleost marine species, Sci. Total Environ. 644 (2018) 1323–1335.
[41] F. Yin, P. Sun, B. Tang, X. Dan, A. Li, Immunological, ionic and biochemical responses in blood serum of the marine fish Trachinotus ovatus to poly-infection by Cryptocaryon irritans, Exp. Parasitol. 154 (2015) 113–117.
[42] P.J. Burgess, R.A. Matthews, Cryptocaryon irritans(Ciliophora): acquired protective immunity in the thick-lipped mullet, Chelon labrosus 5 (1995) 459–468.
[43] C. Guo, B. Peng, M. Song, C.W. Wu, M.J. Yang, J.Y. Zhang, et al., Live *Edwardsiella tarda* vaccine enhances innate immunity by metabolic modulation in zebrafish, Fish Shellfish Immunol. 47 (2015) 664–673.
[44] Y. Li, F. Zhou, J. Huang, L. Yang, S. Jiang, Q. Yang, et al., Transcriptome reveals involvement of immune defense, oxidative imbalance, and apoptosis in ammonia-stress response of the black tiger shrimp (Penaeus monodon), Fish Shellfish Immunol. 83 (2018) 162–170.
[45] J. Marcinkiewicz, E. Kontny, Taurine and inflammatory diseases, Amino Acids 46 (2014) 7–20.
[46] J.E. Seegmiller, T. Watanabe, M.H. Shreier, T.A. Waldmann, Immunological aspects of purine metabolism, Adv. Exp. Med. Biol. 76A (1977) 412–433.
[47] B.P. Lawrence, N.I. Kerkvliet, Role of altered arachidonic acid metabolism in 2,3,7,8-tetrachlorodibenzo-p-dioxin-induced immune suppression in C57Bl/6 mice, Toxicol. Sci. : Off. J. Soc. Toxicol. 42 (1998) 13–22.
[48] J. Chen, Y. Xu, Q. Han, Y. Yao, H. Xing, X. Teng, Immunosuppression, oxidative stress, and glycometabolism disorder caused by cadmium in common carp (Cyprinus carpio L.): application of transcriptome analysis in risk assessment of environmental contaminant cadmium, J. Hazard Mater. 366 (2019) 386–394.
[49] N.C. Williams, L.A.J. O'Neill, A role for the krebs cycle intermediate citrate in metabolic reprogramming in innate immunity and inflammation, Front. Immunol. 9 (2018) 141.
[50] A. Chen, C. Singh, G. Oikonomou, D.A. Prober, Genetic analysis of histamine signaling in larval zebrafish sleep, eNeuro 4 (2017).
[51] G.A. Castro, Intestinal physiology in the parasitized host: integration, disintegration, and reconstruction of systems, Ann. N. Y. Acad. Sci. 664 (1992) 369–379.
[52] C.-K. Khoo, A.M. Abdul-Murad, B.-C. Kua, A. Mohd-Adnan, *Cryptocaryon irritans* infection induces the acute phase response in Lates calcarifer: a transcriptomic perspective, Fish Shellfish Immunol. 33 (2012) 788–794.
[53] P.G. Barbalho, I. Lopes-Cendes, C.V. Maurer-Morelli, Indomethacin treatment prior to pentylenetetrazole-induced seizures downregulates the expression of il1b and cox2 and decreases seizure-like behavior in zebrafish larvae, BMC Neurosci. 17 (2016) 12.
[54] C. Dube, A. Vezzani, M. Behrens, T. Bartfai, T.Z. Baram, Interleukin-1beta contributes to the generation of experimental febrile seizures, Ann. Neurol. 57 (2005) 152–155.
[55] K.A. Sharkey, Substance P and calcitonin gene-related peptide (CGRP) in gastrointestinal inflammation, Ann. N. Y. Acad. Sci. 664 (1992) 425–442.
[56] J.D. Biller-Takahashi, E.C. Urbinati, Fish Immunology. The modification and manipulation of the innate immune system: Brazilian studies, An. Acad. Bras. Cienc. 86 (2014) 1484–14506.
[57] P. Hunter, The inflammation theory of disease. The growing realization that chronic inflammation is crucial in many diseases opens new avenues for treatment, EMBO Rep. 13 (2012) 968–970.
[58] N. Chabane, N. Zayed, M. Benderdour, J. Martel-Pelletier, J.P. Pelletier, N. Duval, et al., Human articular chondrocytes express 15-lipoxygenase-1 and -2: potential role in osteoarthritis, Arthritis Res. Ther. 11 (2009) R44.
[59] G. Burnstock, Purinergic signaling and vascular cell proliferation and death, Arterioscler. Thromb. Vasc. Biol. 22 (2002) 364–373.
[60] P. Illes, J. Alexandre Ribeiro, Molecular physiology of P2 receptors in the central nervous system, Eur. J. Pharmacol. 483 (2004) 5–17.
[61] C. Cekic, J. Linden, Purinergic regulation of the immune system, Nat. Rev. Immunol. 16 (2016) 177–192.
[62] M.D. Baldissera, C.F. Souza, R.C.V. Santos, B. Baldisserotto, Purinergic system displays an anti-inflammatory profile in serum of silver catfish experimentally infected with *Streptococcus agalactiae*: an attempt to ameliorate the inflammatory response, Microb. Pathog. 114 (2018) 193–196.
[63] C.A. Iregui, J. Comas, G.M. Vasquez, N. Verjan, Experimental early pathogenesis of *Streptococcus agalactiae* infection in red tilapia Oreochromis spp, J. Fish Dis. 39 (2016) 205–215.
[64] P.N. Rocha, T.J. Plumb, T.M. Coffman, Eicosanoids: lipid mediators of inflammation in transplantation, Springer Semin. Immunopathol. 25 (2003) 215–227.
[65] M.K. Middleton, A.M. Zukas, T. Rubinstein, M. Kinder, E.H. Wilson, P. Zhu, et al., 12/15-lipoxygenase-dependent myeloid production of interleukin-12 is essential for resistance to chronic toxoplasmosis, Infect. Immun. 77 (2009) 5690–5700.
[66] B.A. Evans, C. Elford, A. Pexa, K. Francis, A.C. Hughes, A. Deussen, et al., Human osteoblast precursors produce extracellular adenosine, which modulates their secretion of IL-6 and osteoprotegerin, J. Bone Miner. Res. : Off. J. Am. Soc. Bone

Miner. Res. 21 (2006) 228–236.
[67] I.C. Iser, P.A. Bracco, C.E. Goncalves, R.F. Zanin, N.B. Nardi, G. Lenz, et al., Mesenchymal stem cells from different murine tissues have differential capacity to metabolize extracellular nucleotides, J. Cell. Biochem. 115 (2014) 1673–1682.
[68] G. Burnstock, P2X ion channel receptors and inflammation, Purinergic Signal. 12 (2016) 59–67.
[69] L. Zhang, Y. Qi, Z.A.L., S. Liu, Z. Zhang, L. Zhou, Betaine increases mitochondrial content and improves hepatic lipid metabolism, Food & function 10 (2019) 216–223.
[70] B. Zabaras-Krick, Betaine improves energy utilisation, Intern Pig Top 12 (1997) 12–14.
[71] N. Kumar, S. Gupta, N.K. Chandan, M. Aklakur, A.K. Pal, S.B. Jadhao, Lipotropes protect against pathogen-aggravated stress and mortality in low dose pesticide-exposed fish, PLoS One 9 (2014) e93499.
[72] H. Sano, M. Imokawa, R. Sager, Detection of heavy methylation in human repetitive DNA subsets by a monoclonal antibody against 5-methylcytosine, Biochim. Biophys. Acta 951 (1988) 157–165.
[73] K.C. Klasing, K.L. Adler, J.C. Remus, C.C. Calvert, Dietary betaine increases intraepithelial lymphocytes in the duodenum of coccidia-infected chicks and increases functional properties of phagocytes, J. Nutr. 132 (2002) 2274–2282.
[74] K.S. Ovington, L.M. Alleva, E.A. Kerr, Cytokines and immunological control of Eimeria spp, Int. J. Parasitol. 25 (1995) 1331–1351.
[75] M. Abdel-Tawwab, M.N. Monier, Stimulatory effect of dietary taurine on growth performance, digestive enzymes activity, antioxidant capacity, and tolerance of common carp, *Cyprinus carpio* L., fry to salinity stress, Fish Physiol. Biochem. 44 (2018) 639–649.
[76] R.H. Fetterer, P.C. Augustine, P.C. Allen, R.C. Barfield, The effect of dietary betaine on intestinal and plasma levels of betaine in uninfected and coccidia-infected broiler chicks, Parasitol. Res. 90 (2003) 343–348.
[77] Ciro Alberto de Oliveira Ribeiro, Alberto Katsumiti, Patrícia França, Jocieli Maschio, Eliandra Zandoná, Marta Margarete Cestari, et al., Biomarkers responses in fish (Atherinella brasiliensis) of paranaguá bay, southern Brazil, for assessment of pollutant effects, Braz. J. Oceanogr. 61 (2013) 1–14.
[78] A. Katsumiti, F.X. Domingos, M. Azevedo, M.D. da Silva, R.C. Damian, M.I. Almeida, et al., An assessment of acute biomarker responses in the demersal catfish Cathorops spixii after the Vicuna oil spill in a harbour estuarine area in Southern Brazil, Environ. Monit. Assess. 152 (2009) 209–222.
[79] R.P. Ellis, J.I. Spicer, J.J. Byrne, U. Sommer, M.R. Viant, D.A. White, et al., (1)H NMR metabolomics reveals contrasting response by male and female mussels exposed to reduced seawater pH, increased temperature, and a pathogen, Environ. Sci. Technol. 48 (2014) 7044–7052.
[80] K. Fumi, H.N., J.O.B. Kjersti Ga, Antiparasitic effect of dietary Romet®30 (SDMX–OMP) against ciliate *Cryptocaryon irritans* infection in the red sea bream *Pagrus major* and tiger puffer *Takifugu rubripes*, Aquaculture 344–349 (2012) 35–39.
[81] F. Yin, Q. Gong, Y. Li, X. Dan, P. Sun, Q. Gao, et al., Effects of *Cryptocaryon irritans* infection on the survival, feeding, respiratory rate and ionic regulation of the marbled rockfish *Sebastiscus marmoratus*, Parasitology 141 (2014) 279–286.
[82] P. Li, K. Mai, J. Trushenski, G. Wu, New developments in fish amino acid nutrition: towards functional and environmentally oriented aquafeeds, Amino Acids 37 (2009) 43–53.
[83] J.T. Brosnan, Glutamate, at the interface between amino acid and carbohydrate metabolism, J. Nutr. 130 (2000) 988S-90S.
[84] M.J. Gibala, Regulation of skeletal muscle amino acid metabolism during exercise, Int. J. Sport Nutr. Exerc. Metab. 11 (2001) 87–108.
[85] A.A. Boldyrev, D.O. Carpenter, P. Johnson, Emerging evidence for a similar role of glutamate receptors in the nervous and immune systems, J. Neurochem. 95 (2005) 913–918.
[86] M.I. Amores-Sanchez, M.A. Medina, Glutamine, as a precursor of glutathione, and oxidative stress, Mol. Genet. Metab. 67 (1999) 100–105.
[87] A.T. ohnson, Y. Kaufmann, S. Luo, K. Babb, R. Hawk, V.S. Klimberg, Gut glutathione metabolism and changes with 7,12-DMBA and glutamine, J. Surg. Res. 115 (2003) 242–246.
[88] I. Roznere, G.T. Watters, B.A. Wolfe, M. Daly, Nontargeted metabolomics reveals biochemical pathways altered in response to captivity and food limitation in the freshwater mussel *Amblema plicata*, Comp. Biochem. Physiol. Genom. Proteonom. 12 (2014) 53–60.